

## ELEVATED LEVELS OF PETITE FORMATION IN STRAINS OF *SACCHAROMYCES CEREVISIAE* RESTORED TO RESPIRATORY COMPETENCE. II. ORGANIZATION OF MITOCHONDRIAL GENOMES IN STRAINS HAVING HIGH AND MODERATE FREQUENCIES OF PETITE MUTANT FORMATION

R. J. EVANS<sup>1</sup> AND G. D. CLARK-WALKER

*Department of Genetics, Research School of Biological Sciences, The Australian National University, Canberra, A.C.T. 2601, Australia*

Manuscript received April 15, 1984

Revised copy accepted July 6, 1985

### ABSTRACT

Restriction enzyme analysis of aberrant mtDNA molecules in restored strains of *Saccharomyces cerevisiae* that display an elevated level of petite formation has shown the occurrence of novel junction fragments and nonstoichiometric amounts for some unaltered bands. Five aberrant mitochondrial genomes from high-frequency petite-forming (hfp) strains (>60% petites per generation) contain like-oriented duplications and single copy regions. High-frequency petite formation is postulated to arise from increased intramolecular recombination between duplicated segments. Mitochondrial DNA structures in two other hfp strains cannot be easily interpreted and might arise from intramolecular recombination.—Mitochondrial DNA from moderate-frequency petite-forming (mfp) strains (5–16% petites per generation) contains inverted duplications in two cases. The elevated petite formation is postulated to arise from homologous recombination between directly repeated sequences. In mtDNA from one mfp strain, deletion end-points have been shown to overlap. Such deletion end-point overlap is postulated to be required for the maintenance of the tandem duplication in hfp strains. Two regions of the wild-type mtDNA (between *cyb* and *oli2* and between SrRNA and *oxi2*) appear to be dispensable for mitochondrial function.

GENETIC studies with spontaneous, respiratory deficient, petite mutants of *Saccharomyces cerevisiae* have shown that respiratory competent colonies can be obtained on crossing recently arisen mutants (CLARK-WALKER and MIKLOS 1975). Subsequently, it has been found that some of the restored forms produced a higher than normal frequency of petite mutants (OAKLEY and CLARK-WALKER 1978). In a more detailed study it has been shown that restored forms, producing elevated numbers of petite mutants, can be separated into those that have a mutational frequency of >60% (high-frequency petite-

<sup>1</sup> Present address: CSIRO Division of Molecular Biology, P.O. Box 184, North Ryde, Sydney, N.S.W. 2113, Australia.

forming, hfp) and those that show a moderate frequency of 5–16% (mfp) (see accompanying paper, EVANS, OAKLEY and CLARK-WALKER 1985). Examination of mtDNA from both hfp and mfp strains by restriction endonuclease analysis has shown that these strains invariably contain aberrant mitochondrial genomes that differ from the wild-type mtDNA by the presence of novel bands, by loss of one or more fragments and by nonstoichiometric levels of some segments (EVANS, OAKLEY and CLARK-WALKER 1985). Our initial interpretation of these results was that the mitochondrial genome in such strains had arisen by recombination between two deleted but complementary molecules and that the product had a duplicated region. It was hypothesized that there could be some relationship between the size of the duplication in the aberrant mtDNA and the frequency of petite mutant formation; however, it was found that there is no simple correlation between the estimated size of the mtDNA duplication and the frequency of petite mutants. For example, two mfp strains, showing petite frequencies of <10%, apparently contain larger duplications [32 and 49 kilobase pairs (kbp)] than an hfp strain (19 kbp) with a frequency of 75% (EVANS, OAKLEY and CLARK-WALKER 1985). This result indicated that factors other than duplication length must be more influential in raising the frequency of petite mutation. We were interested, therefore, in trying to unravel the underlying factors that contribute to the elevated petite mutation rate. The detailed mapping studies of selected representatives of hfp and mfp strains, described in this report, have shown that they differ fundamentally in mitochondrial genome structure. The two observed classes of mitochondrial genome organization provide a basis for a model to explain the frequency of petite mutant formation in the hfp and mfp strains.

#### MATERIALS AND METHODS

*Yeast strains:* The isolation of sectored respiratory competent yeasts resulting from mating recently arisen petites of *S. cerevisiae* (strains D13.1A and T3/3) has been described (see accompanying paper, EVANS, OAKLEY and CLARK-WALKER 1985). For details of the strains used in this study refer to table 1 of that paper.

*Procedures:* Procedures for isolating and characterizing mtDNA are described in the accompanying paper (EVANS, OAKLEY and CLARK-WALKER 1985). For the current series of experiments the pAN124 marker fragments were supplemented with the 30.3- and 17.5-kbp  $\lambda$ c72 *Kpn*I fragments (DANIELS, SCHROEDER and BLATTNER 1980) and the 0.9- and 0.66-kbp pBR322 *Alu*I fragments (SUTCLIFFE 1978). TA buffer (O'FARRELL, KUTTER and NAKANISHI 1980), which replaced the individual restriction endonuclease digestion buffers, proved satisfactory for the restriction endonucleases *Bam*HI, *Bgl*II, *Cla*I, *Hha*I, *Hpa*I, *Pvu*II, *Sac*I, *Sal*I, *Sph*I and *Xho*I, although loss of specificity was observed in digests of dA:dT-rich DNA with *Eco*RI and *Bcl*I. Restriction endonucleases *Bam*HI, *Hha*I, *Sal*I and *Sph*I were produced locally according to the method of GREENE *et al.* (1978). *Bgl*II, *Cla*I, *Hpa*I, *Pvu*II and *Xho*I were supplied by Boehringer Mannheim, West Germany. *Sac*I was obtained from New England Biolabs, Beverly, Massachusetts. Densitometric scans were performed on photographic negatives of the electrophoretically separated restriction fragments, using an LKB 2202 Ultrosan laser densitometer. In order to minimize the difficulties associated with saturation of the silver grain over particularly bright bands, the photographic negatives used for densitometry were slightly underexposed.

Transfer of electrophoretically separated DNA fragments to nitrocellulose filters, <sup>32</sup>P labeling of probes, DNA-DNA hybridization methods and autoradiography have been described (CLARK-

TABLE 1

*Probes used in hybridization analysis of D13.1A mtDNA*

Locus	Probe	Size (kbp) of mtDNA retained	Reference
LrRNA	68-4-2	~4.5	ATCHISON <i>et al.</i> (1979)
<i>oxi1</i>	pSCM5	~2.5	CLARK-WALKER, MCARTHUR and SRIPRAKASH (1983)
<i>oxi2</i>	DS31	~4.5	THALENFELD and TZAGOLOFF (1980)
SrRNA	P2	~5.5	SOR and FUKUHARA (1980)
<i>oxi3</i> (exons 1-3)	DS6/A401	~6.1	BONITZ <i>et al.</i> (1980)
<i>oxi3</i> (exons 3-8)	DS6/A422	~5.3	BONITZ <i>et al.</i> (1980)
<i>oli2</i>	DS14	~4.1	MACINO and TZAGOLOFF (1980)
<i>cyb</i> (exon 1)	DS400/N1	~0.4	NOBREGA and TZAGOLOFF (1980)
<i>cyb</i> (exon 3)	DS400 M11	~3.4	NOBREGA and TZAGOLOFF (1980)
<i>oli1</i>	DS400/A3	~1.8	MACINO and TZAGOLOFF (1979)
<i>var1</i>	pBRvar1	~1.0	HUDSPETH <i>et al.</i> (1982)

WALKER *et al.* 1980; CLARK-WALKER and SRIPRAKASH 1981). The probes used are shown in Table 1.

## RESULTS

*Construction of mitochondrial DNA map of the parental grande strains:* As a prerequisite for the analysis of the abnormal mitochondrial genomes in sectored restored strains, it was necessary to have an accurate map of the restriction endonuclease sites in the parental mtDNA from strain D13.1A. A restriction endonuclease map of the mitochondrial DNA present in isomitochondrial strains D13.1A and T3/3 was constructed by standard methods (Figure 1). (For details see EVANS 1983.) Genic regions were identified by employing specific cloned fragments of mtDNA (Table 1) in hybridization experiments. Precise placements of these probes were made by alignment of the D13.1A restriction sites with the corresponding enzyme recognition sequence in the published data for the probes. To our knowledge, the 81 kbp mitochondrial genome of *S. cerevisiae* strain D13.1A is the largest so far reported.

*Structure of the mitochondrial genome in [1]9.6s3:* In the accompanying report (EVANS, OAKLEY and CLARK-WALKER 1985), consensus values for mitochondrial genome size could be obtained for only two hfp strains, [1]9.6s3 and [1]9.15s, that were shown to have identical restriction endonuclease fragmentation patterns. In the expectation that the mitochondrial genome(s) of these two strains would be the least complex to analyze, we commenced our investigations with mtDNA from [1]9.6s3 as an arbitrarily chosen representative of both genomes.

Our method for investigating the structure of the mitochondrial genome in this strain has been to determine, by a series of restriction endonuclease digestions, the fragments retained or lost from the aberrant mtDNA by comparison with the wild-type mtDNA. We have also examined by densitometry the relative amount of each fragment in restriction digests, as we expected that novel

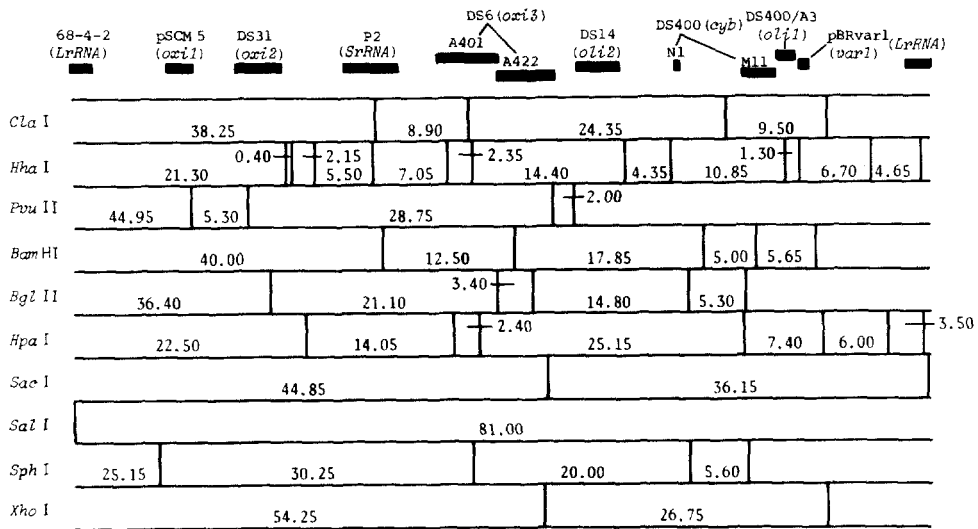


FIGURE 1.—Completed restriction endonuclease map of the mitochondrial genome of *S. cerevisiae* strain D13.1A linearized at the unique *Sal*I site. The positions of the probes to genic regions of the mtDNA are shown above the map. Their precise locations were established by alignment of D13.1A restriction endonuclease sites with corresponding sites reported in the map and sequence data available for the probes (see Table 1).

fragments should be present in single copy and that unaltered fragments should be present in either single or double copy. These predictions are based on the belief that, in the simplest case, restoration to respiratory function results from recombination between defective mtDNA molecules to produce a new molecule having both unique and duplicated regions and two novel junctions (OAKLEY and CLARK-WALKER 1978).

Fragments produced by digestion of [1]9.6s3 mtDNA with several restriction enzymes are shown in Figure 2a, and sizes of these fragments are listed in Table 2. In addition, a densitometric scan of the *Hha*I-produced fragments was obtained, as shown in Figure 3b. The ratios of the fragments found by this method are approximately 1:2 with the two novel fragments present in single copy.

The presence, absence or duplication of particular bands in the five separate digests were scored with respect to the wild-type restriction map (Figure 4a). Sizes of novel bands are listed at the side of the figure. The data in Table 2 and Figure 4a have been used to construct maps of the two participating defective molecules before recombination. Diagrams illustrating the position and extent of the deletions in the two molecules (labeled  $\alpha$  and  $\beta$ ) are shown in Figure 4b and have been deduced according to the following pathway.

It can be seen from Figure 4a that bands corresponding to wild-type fragments, which have been scored as duplications, lie adjacent to each other on the wild-type restriction map. This finding supports the belief that these bands come from a duplicated region, rather than resulting from fortuitous comigration of new fragments.

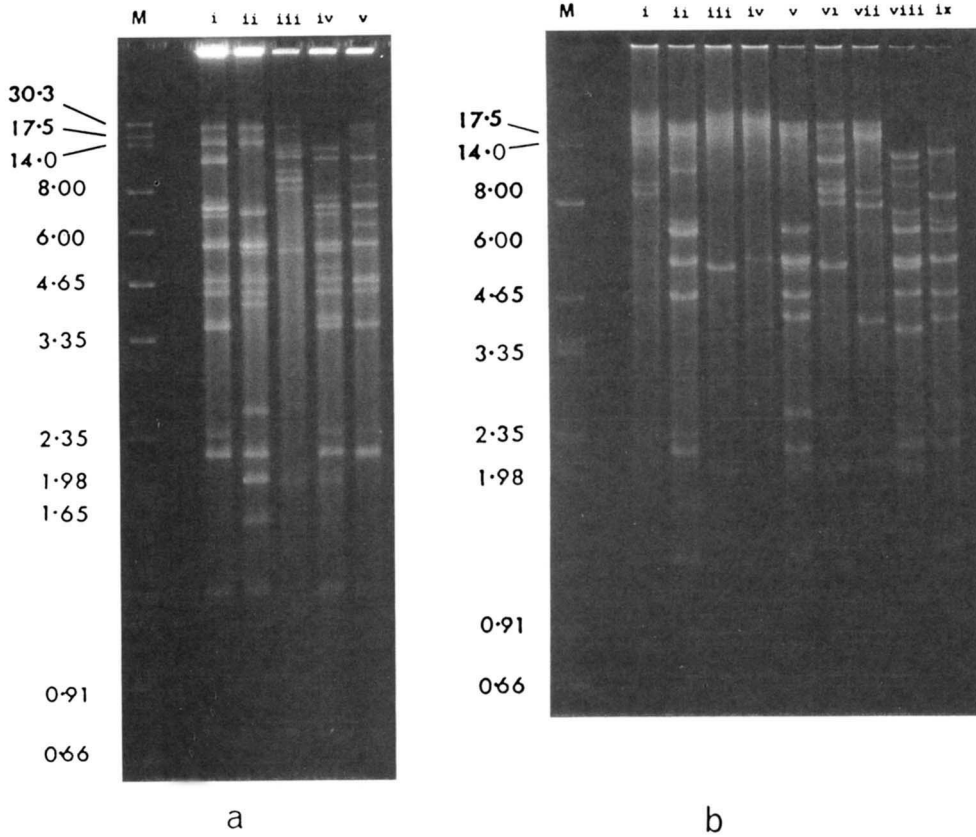


FIGURE 2.—Electrophoresis in 0.8% agarose gels of mtDNA from hfp and mfp strains digested with restriction endonucleases. A series of marker fragments are included in channels labeled M, and their sizes given (in kbp) to the left. a, mtDNA from hfp strain [1]9.6s3 digested with (i) *HhaI*, (ii) *ClaI/HhaI*, (iii) *ClaI/PvuII*, (iv) *HhaI/PvuII* and (v) *HhaI/XhoI*; b, mtDNA from mfp strain [1]9.6s5 digested with (i) *ClaI*, (ii) *HhaI*, (iii) *PvuII*, (vi) *SphI*, (v) *ClaI/HhaI*, (vi) *ClaI/PvuII*, (vii) *ClaI/SphI*, (viii) *HhaI/PvuII* and (ix) *HhaI/SphI*.

Single-copy restriction bands, which are also present, must have been contributed intact to the hfp mitochondrial genome by only one of the parental defective molecules, as they have been either partly or entirely deleted in the mtDNA from the other parent. In addition, the diagram in Figure 4a shows that restriction fragments are absent from one region of the map that is confined to the 4.8-kbp *HhaI-PvuII* fragment.

Based on our initial model for hfp genomes, there should be four deletion end-points identified by loss of restriction endonuclease fragments. By using a number of restriction endonuclease digests, it should be possible to determine the approximate location of these end-points. If duplicated fragments are assumed to have been contributed to the mtDNA of the restored strain by both parental petite strains, then the first single-copy fragment lying immediately adjacent to a duplicated region of the restriction map is considered to have been the site of a deletion event in one or other of the defective mitochondrial

TABLE 2

*Sizes of restriction endonuclease fragments from mtDNA of [1]9.6s3*

<i>HhaI</i>		<i>ClaI/HhaI</i>		<i>ClaI/PvuII</i>		<i>HhaI/PvuII</i>		<i>HhaI/XhoI</i>	
A	B	A	B	A	B	A	B	A	B
21.30	1	21.30	1	21.05	1	12.30	1	21.30	1
~14.50*	1	~14.50*	1	13.00*	1	10.85	1	10.85	1
10.85	1	6.90	2	11.90	1	7.60	1	8.10*	1
7.05	2	5.60	1	11.20*	1	7.05	2	7.05	2
6.70	1	5.50	2	9.50	1	6.70	1	6.30	1
5.50	2	5.25	1	8.90	2	5.50	2	5.50	2
4.65	1	4.65	1	7.95	1	5.30	1	4.65	1
4.35	1	4.35	1	5.30	1	4.80*	1	4.55	1
3.60*	1	4.10	1	2.00	1	4.65	1	4.35	1
2.35	1	2.60	1	99.70		4.35	1	3.60*	1
2.15	2	2.15	2			3.70	1	2.35	1
1.30	1	2.00	2			3.60*	1	2.15	2
0.40	(2)	1.60*	1			2.35	1	2.15	1
~99.80		1.30	1			2.15	2	1.30	1
		0.40	(2)			2.00	1	0.40	(2)
		0.35	(1)			1.30	1	99.70	
		0.15	(2)			0.40	(2)		
		~99.80				99.70			

Fragment sizes, in kbp, are shown in column A, and relative band stoichiometries determined by densitometry are given in column B. Novel fragments are marked as \*, and parentheses indicate that the stoichiometries have been estimated from the known map positions of these fragments (relative to regions of established stoichiometry).

genomes. From the diagram in Figure 4a it can be seen that a 2.0-kbp *ClaI-HhaI* fragment is duplicated, whereas the 2.35-kbp *HhaI* fragment from which such a band arises is present in only single copy. This positions one end-point within the 0.35-kbp *ClaI-HhaI* region. A second end-point must be within the 3.7-kbp *HpaI-PvuII* fragment as the left end of the duplication extends to the small 0.40-kbp *HhaI* fragment. A third end-point can be located within the 4.8-kbp *HhaI-PvuII* band that is missing from the digest. The expected fourth end-point also lies within this fragment, but confirmation of this fact had to be obtained through analyzing the junction fragments, as outlined below.

Deletion-associated junction fragments for any digest should correspond to the sum of the distances between the deletion end-point and the nearest restriction site at each end of the simple deletion. By considering the sizes of the junction fragments, it is possible to map the positions of the deletion end-points in the complementing molecules (Figure 4b).

In one defective molecule, the deletion extends rightwards from the 0.35-kbp *HhaI-ClaI* fragment into the 4.8-kbp *HhaI-PvuII* fragment; this deletion results in the creation of a 3.6-kbp *HhaI* junction fragment. Of this junction fragment at least 2.0 kbp and, at most, 2.35 kbp is derived from the 2.35-kbp *HhaI* fragment. This then places the right-hand deletion end-point between 1.6 kbp (3.6 - 2.0) to 1.25 kbp (3.6 - 2.35) from the right end of the 4.8-kbp *HhaI-PvuII* fragment. This placement is confirmed by junction sizes ob-

tained from other digests. Molecule  $\beta$  has therefore sustained a simple deletion of  $((2.35 + 14.4) - 3.6)$  13.15 kbp that has excised the *oxi3* and *oli2* coding regions.

The deletion in molecule  $\alpha$  extends from a position within the 4.8-kbp *HhaI-PvuII* fragment rightwards to the 3.7-kbp *HhaI-PvuII* fragment. In the *HhaI/PvuII* digest there is a 4.8-kbp junction fragment. In the two extreme cases, such a fragment could comprise all of the *HhaI-PvuII* 4.8-kbp wild-type fragment and very little of the 3.7-kbp *HhaI-PvuII* fragment or, alternatively, all of the 3.7-kbp *HhaI-PvuII* fragment and  $(4.8 - 3.7)$  1.1 kbp of the 4.8-kbp *HhaI-PvuII* fragment. The deletion resulting in either case (by addition of the *PvuII* or *HhaI-PvuII* fragments lost, minus the junction fragment size) is  $((44.95 + 5.3 + 3.7) - 4.8)$  49.15 kbp. This includes the coding regions of *cyb*, *oli1*, *var1*, LrRNA, *oxi1* and *oxi2*. Although the deletion does not extend into the *oli2* region, we believe that the deletion end-point in this region overlaps with the right deletion end-point in the  $\beta$  petite (as discussed below).

Thus, we have been able to construct maps for the two hypothetical deleted molecules that, together, comprise the mitochondrial genome of [1]9.6s3 (Figure 4b). Furthermore, we believe that the mitochondrial genome of strain [1]9.15s, because it has an identical fragmentation pattern to [1]9.6s3, is composed of similarly deleted molecules.

*Structure of the mitochondrial genome of hfp strains [1]15.19s, [2]13.10s and [2]17.5s:* When mtDNA restriction fragments from various digests of hfp strains other than [1]9.6s3 and [1]9.15s were classified by eye as being duplicated or present in single copy, it was found that consensus values for mtDNA size could not be obtained.

Densitometric scans of electrophoretically separated restriction fragments for strains [1]15.19s, [2]13.10s and [2]17.5s (Figure 3c-e) have allowed their true stoichiometric relationships to be established. After making allowance for differential fluorescence and yield of fragments, as well as for comigration of certain bands, it was found that triplications were present in addition to the duplicated and single copy bands.

The simplest interpretation of this information is that the two defective mtDNA molecules in some restored strains are not present in equal amounts. Under circumstances where one molecule is present at twice the level of the other, single copy bands would be contributed only by the underrepresented molecule and "duplicated" bands by the overrepresented molecule, whereas "triplicated" fragments are contributed by both defective genomes. The absolute stoichiometries would be dependent on the level of overrepresentation of one of the molecules in the isolated mtDNA.

In each case, when the restriction fragment data for strains [1]15.19s, [2]13.10s and [2]17.5s were interpreted on a model involving overrepresentation of one defective molecule, it was possible to construct maps for the parental petites that were participating in the complementation. The level of overrepresentation was estimated as the ratio of the peak areas for "single copy" fragments (molecule  $\alpha$ -derived) and "duplicated" fragments (molecule  $\beta$ -derived); this value varied according to strain.

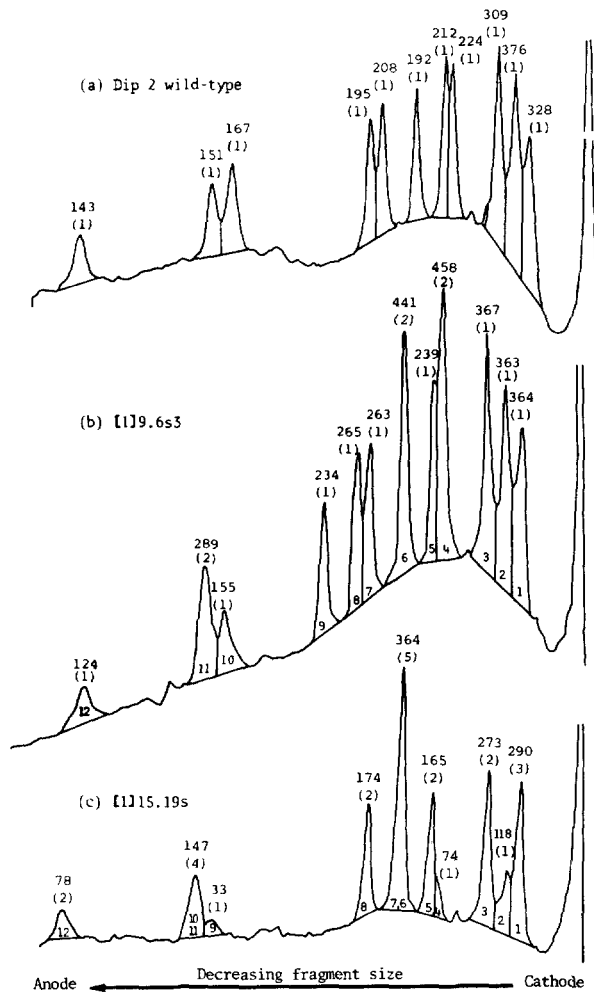


FIGURE 3.—Densitometric scans for *Hha*I-digested mtDNA from wild-type strain Dip2 (a) and hfp strains [1]9.6s3 (b), [1]15.19s (c), [2]13.10s (d), and [2]17.5s (e) after resolution of the fragments by electrophoresis on agarose gels. The numbers within each peak identify the restriction fragment (see Table 2 and Appendixes 1–3). Base lines and peak boundaries were drawn as shown in the figure, and the areas under the peaks measured on a Kontron MOP-AM O3 image analyzer. The values obtained are shown above the peaks. The approximate relative stoichiometries (with allowance made for gel position) are shown in parentheses. The fragments in the digest of wild-type mtDNA are present in close to stoichiometric amounts, the deviation from exact stoichiometry being attributable to a combination of an increasing amount of bound ethidium with increasing fragment size and a lower yield of high molecular weight fragments.

In constructing the maps, similar principles to those used in establishing the parental petite maps of strain [1]9.6s3 were applied to the restriction fragment data given in the Appendix. The completed maps are shown in Figure 5; full details of the mapping procedures are given elsewhere (EVANS 1983).

*Structure of the mitochondrial genome in [1]9.6s5: Investigation of aberrant*



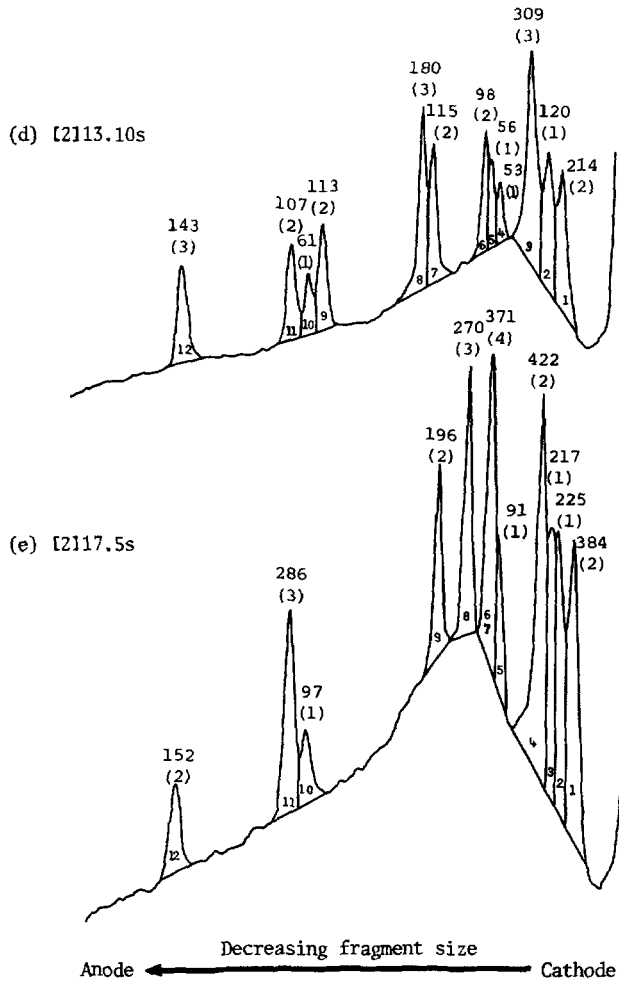


FIGURE 3.—Continued

mtDNA structure in mfp strains was commenced with [1]9.6s5, as initial investigation indicated that a consensus duplication size could be obtained for this mitochondrial genome (see EVANS, OAKLEY and CLARK-WALKER 1985). Accordingly, mtDNA from this strain was subjected to analysis with restriction endonucleases, and digests critical in establishing the map are shown in Figure 2b. Fragment sizes are shown in Table 3; densitometric scans of the restriction fragments (not illustrated) indicated an exact 2:1 stoichiometry of brighter bands with respect to the fainter bands.

The presence, absence or duplication of particular bands was scored with respect to the wild-type restriction map and sizes of novel bands noted (Figure 6a). This information was analyzed on the assumption that junctions had arisen by simple deletion events from circular molecules, as observed for the hfp strains. Initially, we attempted to reconstruct the form of the defective mole-

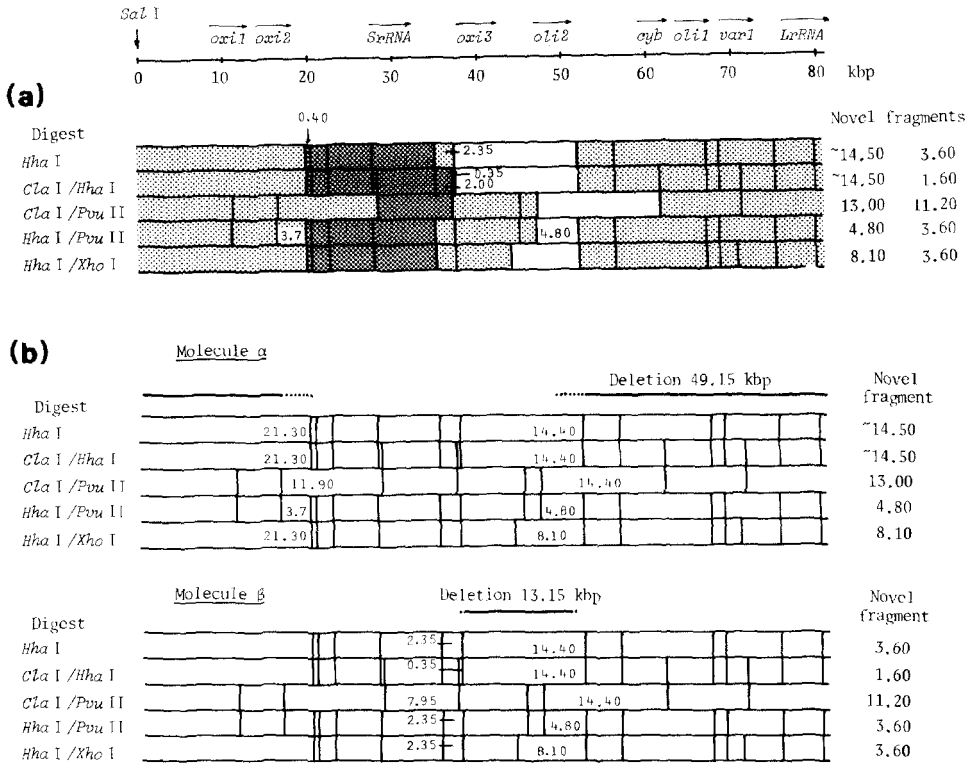


FIGURE 4.—a, Loss/retention map for the mtDNA of strain [1]9.6s3. The data shown in Table 2 are displayed in this figure with respect to the D13.1A mtDNA map (see Figure 1). The restriction map is linearized at the unique *Sal*I site in the *LrRNA* gene and, from left to right, represents a clockwise orientation. Wild-type fragments are scored as being present in single copy, absent or duplicated. The sizes of the novel bands observed in each of the digests are listed (in kbp) to the right of the corresponding map. Key: ■, duplicated fragment; ▨, single copy fragment; □, fragment absent. b, Maps of the deletions sustained by each of the parental defective mtDNA molecules ( $\alpha$  and  $\beta$ ) involved in the complementation event that yielded strain [1]9.6s3. The extent of the deletions are estimated from junction fragment sizes, as described in the text. Regions that are unequivocally deleted are indicated by a solid line; the dotted extensions indicate regions that may or may not be deleted depending on the location of the deletion within its mapped range.

cles that had participated in the complementation. Deletion end-points in strain [1]9.6s5 mtDNA can be placed in a 6.9-kbp *Cla*I-*Hha*I fragment and a 1.6-kbp *Cla*I-*Sph*I fragment.

The observation that, in certain digests of [1]9.6s5, two juxtaposed wild-type restriction bands are absent indicated that overlapping deletions must be present so that each of the absent fragments is deleted entirely from one parent and is involved in a junction fragment in the other (Figure 7a). An alternative arrangement (Figure 7b) can be precluded, as such a combination of deleted molecules would not lead to restoration of respiratory competence. Nonoverlapping deletion end-points can occur only when a single restriction fragment is absent, although loss of a single band could indicate, alternatively, overlap-

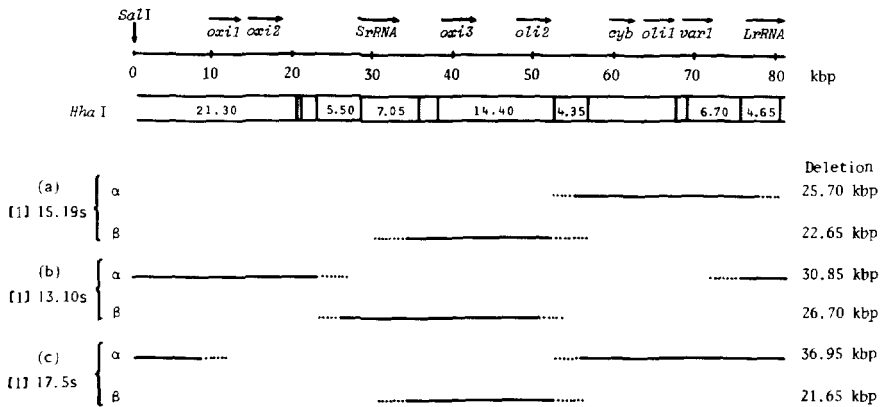


FIGURE 5.—Deletions sustained by each of the parental defective mtDNA molecules involved in the complementation event that yielded strains [1]15.19s, [1]13.10s and [1]17.5s. In each case, the extent of the deletion is estimated from the size of the resulting junction fragment. Regions that are unequivocally deleted are indicated by a solid line; the dotted extensions indicate regions that may or may not be present depending on the location of the deletion end-point within its mapped range. a, [1]15.19s maps: Molecule  $\alpha$  is deleted for *cyb*, *oli1* and *var1* loci and possibly the LrRNA gene. The  $\beta$  molecule has lost a region bearing *oxi3*, *oli2* and possibly SrRNA. There is a probable area of deletion end-point overlap in the 4.35-kbp *HhaI* fragment. A common ~32.7-kbp region is retained that carries the *oxi1*, *oxi2* and LsRNA genes. One defective mtDNA is overrepresented at the level of approximately 2.3:1 (molecule  $\beta$  to molecule  $\alpha$ ). b, [2]13.10 maps: Molecule  $\alpha$  has lost the LrRNA, *oli1* and *oxi2* genes. Molecule  $\beta$  is deleted for a region that includes the coding sequences of SrRNA, *oxi3* and possibly *oli2*. Deletion overlap is located between the *oxi2* and SrRNA genes, and the two defective molecules share a common sequence of ~23.5 kbp that carries *cyb*, *oli1*, *var1* and possibly *oli2*. Molecular  $\beta$  is present at approximately 1.8 times the level of molecule  $\alpha$ . c, [2]17.5s maps: Deletion in molecule  $\alpha$  excises the *cyb*, *oli1*, *var1* and LrRNA loci, but probably does not extend into the *oxi1* locus. The deletion in molecule  $\beta$  results in the loss of *oxi3* and *oli2* and may also affect the SrRNA gene. The common region of ~22.4 kbp carries the *oxi2* locus and possibly the SrRNA and *oxi1* sequences, and it seems probable that there is a region of deletion end-point overlap in the 4.35-kbp *HhaI* fragment. Molecules  $\alpha$  and  $\beta$  of strain [2]17.5s are present in a ratio of approximately 1:2.

ping deletions, where the region of overlap lies entirely within the restriction fragment.

Using the above arguments, a simple deletion in each of the two defective parental mtDNA molecules ( $\alpha$  and  $\beta$ ) of [1]9.6s5 can be drawn that can explain the loss/retention data (Figure 6b). It can be seen that molecule  $\alpha$  has sustained a deletion extending rightwards from the 6.9-kbp *ClaI-HhaI* fragment into the 4.35-kbp *ClaI-HhaI* fragment. Molecule  $\beta$  must have sustained a deletion extending leftwards from the 1.6-kbp *ClaI-SphI* fragment into the 4.8-kbp *HhaI-PvuII* fragment, thereby illustrating that the deletions are overlapping.

The presence of overlapping deletions and the observation of only two novel junction fragments in each digest of mtDNA from [1]9.6s5 supported our initial assumption that the organization of the genome in this strain is similar to that in hfp forms. However, such an arrangement did not give a satisfactory explanation for the observed sizes of junction fragments. Therefore, we considered other possible structures of the mitochondrial genome that could accommodate the junction fragment size data.

TABLE 3  
*Sizes of restriction endonuclease fragments from mtDNA of [119.6s5*

HhaI		ClaI		PvuII		SphI		ClaI/HhaI		ClaI/PvuII		ClaI/SphI		HhaI/PvuII		HhaI/SphI	
A	B	A	B	A	B	A	B	A	B	A	B	A	B	A	B	A	B
21.30	2	large	—	large*	—	—	—	21.30	2	21.05	2	21.00	2	12.30	2	~18.5*	1
~18.5*	1	~18.5*	1	large	—	—	—	~18.5*	1	~16.0*	1	~18.5*	1	10.85	1	12.80	2
10.85	1	~16.0*	1	~21.5*	1	25.15	—	6.90	1	11.90	2	17.25	2	9.00*	1	8.50	2
7.05	1	9.50	1	5.30	2	5.60	1	6.65*	1	9.50	1	8.90	1	7.60	1	7.05	1
6.70	2	8.90	1	2.00	1	3.90*	1	5.60	1	8.90	1	7.90	2	7.05	1	6.70	2
6.65*	1	—	—	—	—	—	—	5.50	2	8.85*	1	4.00	1	6.70	2	5.60	1
5.50	2	—	—	—	—	—	—	5.25	1	7.95	1	3.90*	1	6.65*	1	5.50	2
4.65	2	—	—	—	—	—	—	4.65	2	5.30	2	1.60	1	5.50	2	4.65	2
2.35	1	—	—	—	—	—	—	4.10	2	2.00	1	0.35	(1)	5.30	2	4.00	2
2.15	2	—	—	—	—	—	—	2.60	2	~129.70	—	~129.55	—	4.65	2	2.65*	1
1.30	2	—	—	—	—	—	—	2.15	2	—	—	~129.55	—	3.70	2	2.35	1
0.40	(2)	—	—	—	—	—	—	2.00	1	—	—	—	—	2.35	1	2.15	2
~129.40	—	—	—	—	—	—	—	1.30	2	—	—	—	—	2.15	2	1.30	2
—	—	—	—	—	—	—	—	0.40	(2)	—	—	—	—	2.00	1	1.25	1
—	—	—	—	—	—	—	—	0.35	(1)	—	—	—	—	1.30	2	0.40	(2)
—	—	—	—	—	—	—	—	0.15	(2)	—	—	—	—	0.40	(2)	~129.40	—
—	—	—	—	—	—	—	—	~129.55	—	—	—	—	—	0.40	(2)	~129.40	—
—	—	—	—	—	—	—	—	—	—	—	—	—	—	129.50	—	—	—

See legend to Table 2.

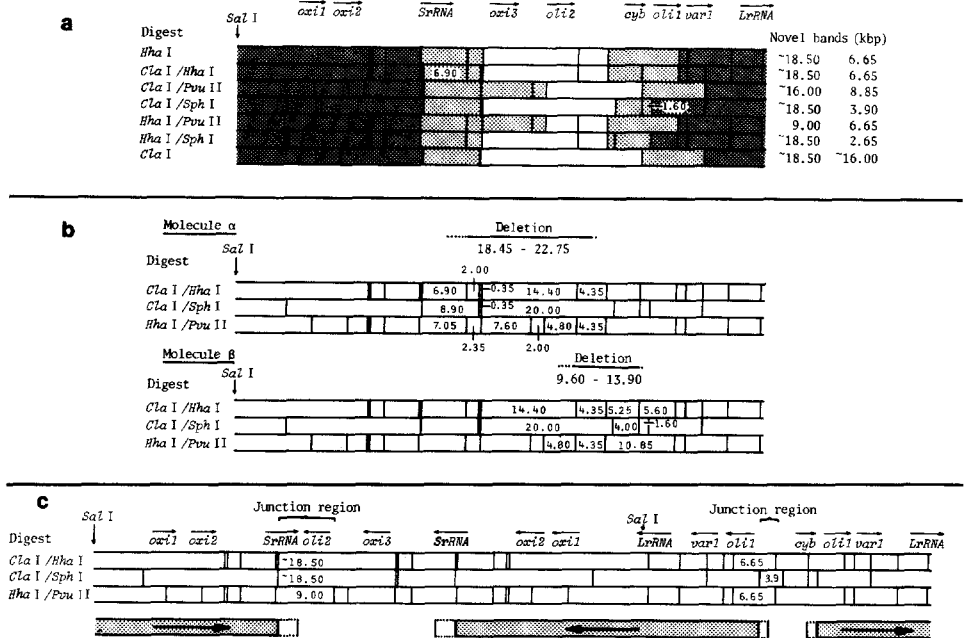


FIGURE 6.—a, Loss/retention map for the mtDNA of strain [1]9.6s5. The data shown in Table 3 are displayed in this figure with respect to the D13.1A mtDNA map. Wild-type fragments are scored as being present in single copy, absent or duplicated. The sizes of the novel bands observed in each of the digests are listed (in kbp) to the right of the corresponding map. Key: duplicated fragment; single copy fragment; fragment absent. b, Putative deletion pattern from parental defective molecules ( $\alpha$  and  $\beta$ ) involved in the formation of mfp strain [1]9.6s5. The extent of the deletions are estimated from junction fragment sizes, as described in the text. The minimum size of deletions are indicated with a solid line, the dotted extensions show the maximum region deleted. c, Mitochondrial genome map for strain [1]9.6s5. The molecule has been formed by an illegitimate recombination between the defective mtDNAs illustrated in b and carries an inverted repeat in the order of 50 kbp. Genomic regions of the molecule and 5'  $\rightarrow$  3' orientation of the coding sequences are indicated. Duplicated parts of the molecule are drawn beneath the map () with the regions of uncertainty (based on the resolution limits of deletion end-point mapping) shown as dotted extensions.

An alternative mechanism for the creation of a novel fragment is illegitimate recombination between two defective mtDNA molecules. In theory, such an event could result in the production of four novel fragments (Figure 8a); however, if illegitimate recombination were to take place via one of the novel junction fragments, only three new bands would be seen (Figure 8b) and, likewise, only two new bands would be present if the site of recombination were to involve both of the original novel fragments (Figure 8c). In this context it must be emphasized that, in every digest of mtDNA from [1]9.6s5, there are only two novel fragments detected, thereby suggesting that the third type of event outlined above has taken place.

In analyzing the data on junction fragment sizes, we were also mindful of the possibility that illegitimate recombination may result in reversed orientation of one portion of the resulting genome. Therefore, we compared the known

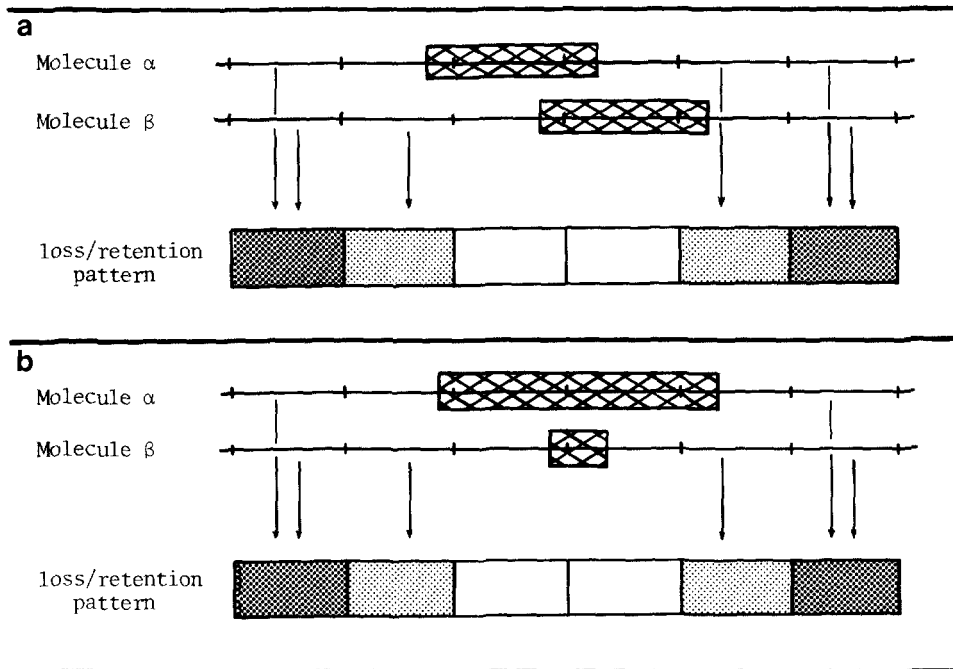
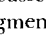
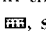
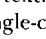
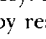


FIGURE 7.—Effect of deletion end-point position on the pattern of restriction fragment loss, retention and duplication. Certain fragments will be retained intact by neither molecule, being either deleted entirely or involved in a deletion-associated junction fragment. The significance of the loss/retention patterns produced by each of the arrangements illustrated to the mapping of mtDNA in mfp strains is discussed in the text. Key: , deletion; , absent restriction fragment; , duplicated restriction fragment; , single-copy restriction fragment;  $\vdash$ , restriction site.

junction fragment data for strain [1]9.6s5 to the expected junction fragment sizes that result from both direct and inverted illegitimate recombination between the putative defective molecules shown in Figure 6b. Absolute fragment lengths could not be compared, as the exact site of recombination within the junctions could not be determined. Differences between novel junction fragment lengths produced by different restriction endonucleases were the critical measurements.

Possible junction fragment sizes that would be detected by *ClaI/SphI* and *HhaI/PvuII* digests of molecules  $\alpha$  and  $\beta$  following illegitimate recombination in both direct and inverted orientation are shown in Figure 9. For simplicity, deletions are shown at their minimum possible size, and the site of illegitimate recombination is taken to be at the original deletion sites. This latter assumption may not be the case in reality; nevertheless, even though both the extent of the deletion event and the site of illegitimate recombination will have a significant effect on the absolute length of the junction fragment created, neither have any effect on the length difference between junction fragments from different digests.

Comparison of predicted and observed junction fragment size differences can be used to determine the orientation of illegitimate recombination as fol-

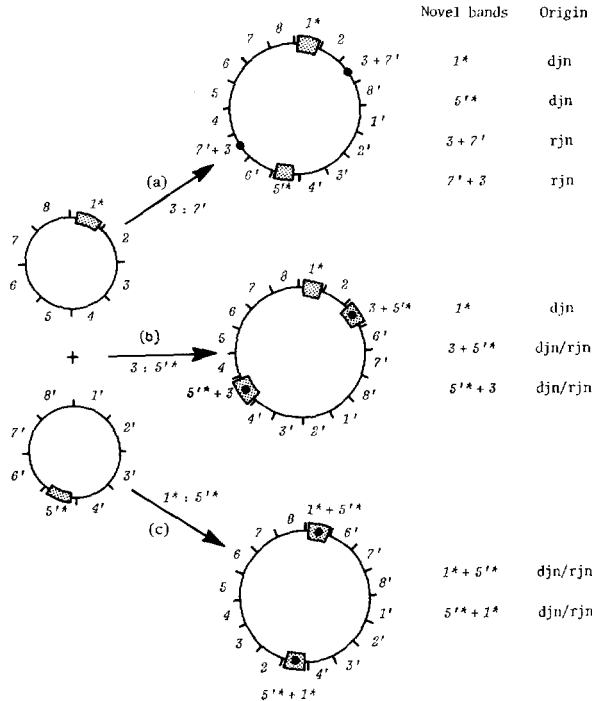


FIGURE 8.—Effect of the position of illegitimate recombination relative to the deletion sites on the number of novel fragments seen in restriction digests. The numbered sectors on the molecules represent restriction fragments. Key: □, deletion; \*, fragment modified by a deletion event; ●, site of illegitimate recombination; ■, illegitimate recombination within a restriction fragment modified by a deletion event; djn, junction fragment created by a deletion event; rjn, junction fragment created by an illegitimate recombination event.

lows. Recombination in direct orientation between the deletion-associated junctions of molecules  $\alpha$  and  $\beta$  brings together the left side of the junction fragment of molecule  $\alpha$  and the right side of the junction fragment of molecule  $\beta$ . Assuming a minimum size for the deletion, *ClaI/SphI* and *HhaI/PvuII* junctions of 8.5 and 12.65 kbp, respectively, would result. Although larger deletions would produce smaller junction fragments, the difference between these junctions would remain the same (4.15 kbp). In the diagram (Figure 9), the difference value is expressed as the *ClaI/SphI* junction size minus the *HhaI/PvuII* junction size, and, hence, a negative difference value is obtained. Recombination in inverted orientation between the deletion-associated junctions of molecules  $\alpha$  and  $\beta$  brings together the right sides of the junction fragments of molecules  $\alpha$  and  $\beta$  and creates *ClaI/SphI* and *HhaI/PvuII* junctions of 7.20 and 9.95 kbp, respectively. The *ClaI/SphI* junction minus *HhaI/PvuII* junction value is -2.75 kbp. No length difference of 4.15 kbp is observed between any two *ClaI/SphI* and *HhaI/PvuII* junctions in digests of [1]9.6s mtDNA; however, a 2.75 kbp difference is observed between the 3.90-kbp *ClaI/SphI* and 6.65-kbp *HhaI/PvuII* junctions. Furthermore, as shown in Figure 9, the differences between the 18.5-kbp *ClaI/SphI* and 9.00-kbp *HhaI/PvuII* junctions

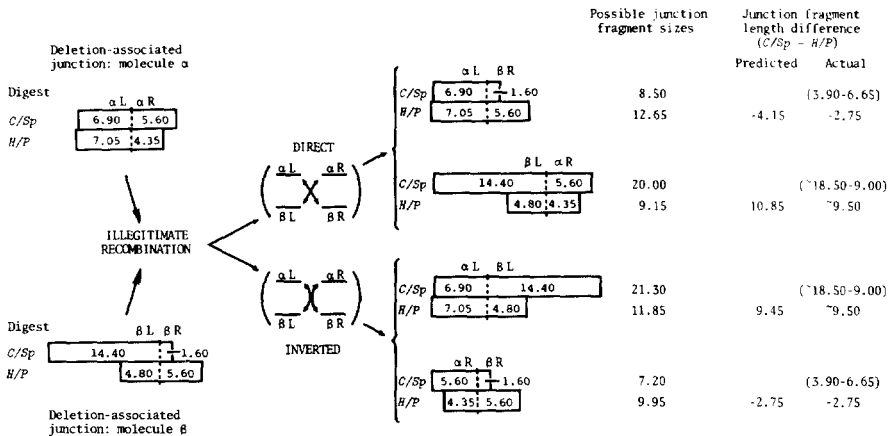


FIGURE 9.—Anticipated effect of illegitimate recombination in both direct and inverted orientation between deletion junction fragments of mfp strain [1]9.6s5. The symbols  $\alpha$  and  $\beta$  identify the defective molecule of origin (see Figure 6b), and deletions are shown at their maximum extents; L and R indicate the left and right flank of the deletion-associated junction fragments. The sizes of the recombinant junctions that would be formed by illegitimate recombination are given in kilobase pairs. A junction length difference between the predicted *ClaI/SphI* and *HhaI/PvuII* novel bands is shown and compared with the actual difference in size between the observed novel bands. Restriction endonuclease names are abbreviated in the diagram: C = *ClaI*, H = *HhaI*, P = *PvuII*, Sp = *SphI*.

agree with those predicted for illegitimate recombination in inverted, but not direct, orientation between the left sides of the deletion-associated junctions of molecules  $\alpha$  and  $\beta$  (Figure 9). Similar agreement was found in junction comparisons from other digests.

It appears that the mitochondrial genome of strain [1]9.6s5 has arisen by illegitimate recombination of the deleted molecules, shown in Figure 6b, between points at or near to their deletion end-points, to create a recombinant molecule carrying a large inverted repeat. More precise placement of the deletion events in the complementing defective molecules was achieved as described below.

The right end of the deletion in molecule  $\beta$  of Figure 6b is known to lie in a 1.6-kbp *ClaI-SphI* fragment. The deletion initiated at this point extends to the 4.8-kbp *HhaI-PvuII* fragment. The junction fragment observed, however, as Figure 9 indicates, is not made up of these two fragments, as exchange has occurred with the other deletion-associated junction fragment. The nondeleted section of the 1.6-kbp *ClaI-SphI* fragment is therefore fused to the remainder of the 4.35-kbp *HhaI-PvuII* fragment at the right-hand end of the molecule  $\alpha$  deletion. The observed junction fragment in the *HhaI/SphI* digest is 2.65 kbp (Figure 6a). Of this, a maximum of 1.6 kbp and a minimum of 0 kbp have been contributed by the *ClaI-SphI* fragment. If recombination occurs between the deletion sites themselves, this places a deletion end-point ((2.65 - 1.6) to (2.65 - 0)) 1.05-2.65 kbp from the right end of the 4.35-kbp *HhaI-PvuII* fragment. If recombination occurs to either side of the deletion points, then some part of the 4.8-kbp *HhaI-PvuII* fragment and/or the 6.9-kbp *ClaI-SphI*



fragment may be included in the junction fragment. In this case, only a maximum contribution (2.65 kbp) can be estimated for the 4.35-kbp *HhaI* fragment. Nonetheless, two deletion end-points have been placed to within 1.6 and 2.65 kbp.

The remaining deletion end-points were located more precisely by the following steps. Part of the 4.8-kbp *HhaI-PvuII* fragment, which contains the left deletion end-point of molecule  $\beta$ , is fused by deletion to the remainder of a 6.9-kbp *ClaI-HhaI* fragment from the left end of the deletion in molecule  $\alpha$ . The 9.0-kbp *HhaI/PvuII* junction indicates that the two primary contributing regions, together, must have lost at least  $((4.8 + 6.9) - 9.0)$  2.7 kbp. By reasoning similar to that used above to place the right-hand deletion end-point in molecule  $\alpha$  and the left-hand deletion end-point in molecule  $\beta$ , it may be deduced that deletion end-points lie 4.2–6.9 kbp from the left end of the 6.9-kbp *ClaI-HhaI* fragment and 2.1–4.8 kbp from the left end of the 4.8-kbp *HhaI-PvuII* fragment (assuming recombination occurred between deletion end-points). If illegitimate recombination occurred between points other than the deletion sites, then the junction must include regions from the 4.35-kbp *HhaI-PvuII* fragment and/or the 1.6-kbp *ClaI-SphI* fragment. If this is the case, then it is not possible to limit the position of the end-points within the deletion-affected parental fragments. More precise placement of the deletion end-points in the complementing mtDNA molecules of strain [1]9.6s5 requires fine structure mapping or nucleotide sequence data; these studies have commenced.

The maps of the parental defective mtDNAs of strain [1]9.6s5, shown in Figure 6b, indicate that molecule  $\alpha$  has sustained a deletion of between 18.45 and 22.75 kbp involving the genes for *oxi3* and *oli2*; molecule  $\beta$  has sustained a deletion of 9.6–13.9 kbp involving the *cyb* gene. The end-points of the deletions overlap, and it is clear that a region of at least 1.7 kbp, lying immediately to the right of the *oli2* locus, is entirely absent from the complemented mitochondrial genome.

The full map of [1]9.6s5 is shown in Figure 6c. Restriction endonuclease analysis of this strain therefore reveals a mitochondrial genome in the order of 130 kbp bearing a 49-kbp (minus overlap) inverted repeat of a region of the genome carrying the genes for *oxi1*, *oxi2*, SrRNA, *oli1*, *var1* and LrRNA. It seems that it has arisen by an illegitimate recombination event between two defective mtDNA molecules  $\alpha$  and  $\beta$  (Figure 6b) that carry simple deletions in the order of 20.5 and 12.0 kbp, respectively.

*Structure of the mitochondrial genome in [1]9.6s4:* Data given in Appendix 4 were used to construct a map of the mitochondrial genome of mfp strain [1]9.6s4, employing the mapping principles established for strain [1]9.6s5. Maps of the parental petites and of the recombinant mfp mitochondrial genome are illustrated in Figure 10.

Molecule  $\alpha$  of strain [1]9.6s4 has suffered a large deletion in the range 39.6–46.0 kbp that has excised the genes for *oli1*, *var1*, LrRNA, *oxi1* and *oxi2*. Molecule  $\beta$  has lost only a small region of 3.65–10.05 kbp that probably contains the gene for the small ribosomal RNA subunit.

It seems possible from the maps of the deletion events in Figure 10a that,

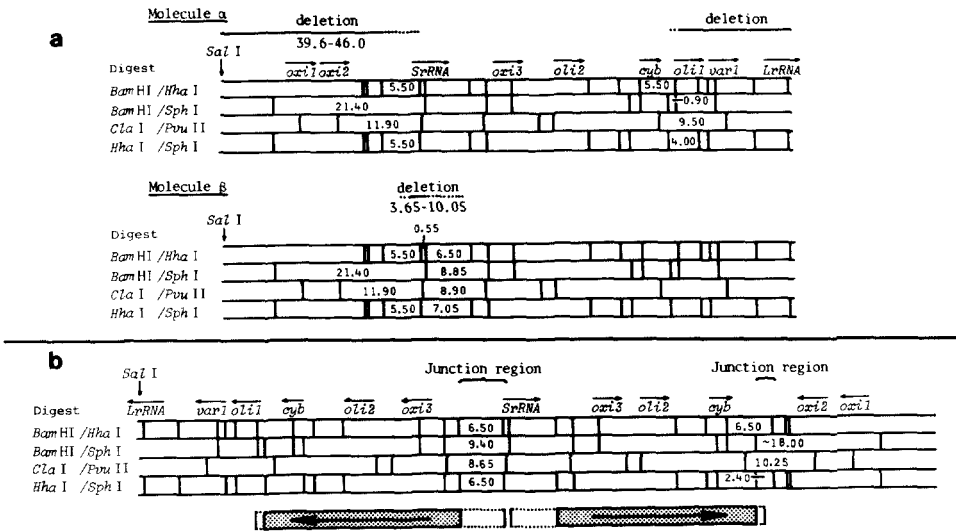


FIGURE 10.—a, Putative deletion pattern from parental defective molecules ( $\alpha$  and  $\beta$ ) involved in the formation of mfp strain [1]9.6s4. The extent of the deletions was estimated from junction fragment sizes, as described for strain [1]9.6s5. The minimum size of deletions is indicated with a solid line, the dotted extensions show the maximum region deleted. b, Mitochondrial genome map for strain [1]9.6s4. The molecule has been formed by an illegitimate recombination between the defective mtDNAs illustrated in a and carries an inverted repeat in the order of 32 kbp. Genomic regions of the molecule and 5'  $\rightarrow$  3' orientation of the coding sequences are indicated. Duplicated parts of the molecule are drawn beneath the map (■), with the regions of uncertainty (based on the resolution limits of deletion end-point mapping) shown as dotted extensions.

in common with [1]9.6s5, strain [1]9.6s4 may also bear an overlap in its deletion end-points. The putative overlap lies in a region of the genome between the small ribosomal RNA gene and the *oxi2* sequence and, presumably, does not include any of the coding sequences for the three tRNAs that are located in this segment.

The size of the mitochondrial genome of this strain is approximately 112.5 kbp, and it contains an inverted duplication of some 32 kbp carrying the *oxi3*, *oli2* and *cyb* loci (Figure 10b). This mtDNA has been generated by illegitimate recombination in an inverted orientation at the two deletion-associated junction fragments. As in the case of strain [1]9.6s5, it has not been possible to establish whether the illegitimate recombination has involved the original deletion sites or adjacent regions.

#### DISCUSSION

The data presented above lead us to the view that the mitochondrial genome in hfp strains is composed of coexisting defective molecules in equilibrium with a recombinant form. Recombination between the two defective forms is envisaged to occur in the shared homologous region, so that the recombinant molecule would contain duplicated sequences in the same orientation. However, we believe that such a molecule is not an intermediate on the pathway toward

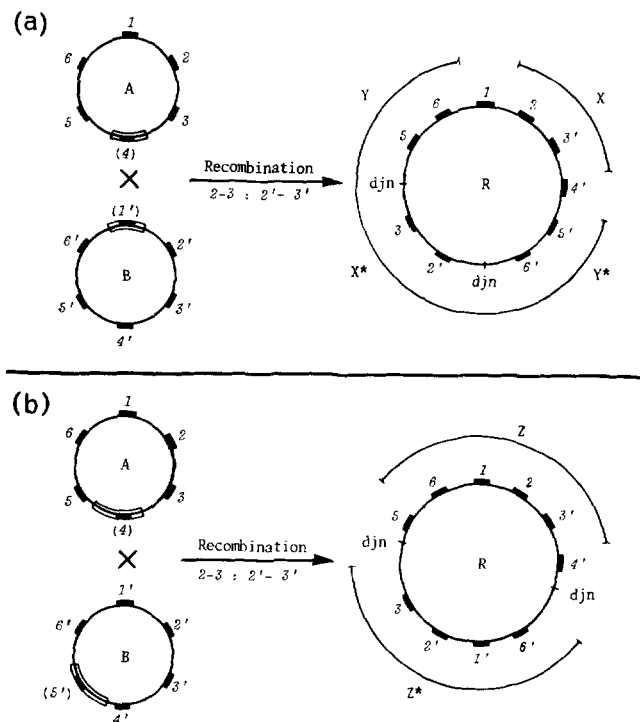


FIGURE 11.—Influence of deletion end-point overlap on possible recombination products. a, If the end-points of the deletions in molecules A and B do not overlap, a recombinant molecule (R) is formed in which there are two possible planes of recombination (X and Y). Intramolecular recombination between X and X\* would reform the parental defective genomes. Alternatively, recombination between Y and Y\* would generate a doubly deleted molecule and a wild-type genome. b, If the deletion end-points in the defective molecules A and B overlap, then the recombinant molecule (R) will have a single possible plane or intramolecular recombination (Z). In consequence, recombination in this molecule could lead only to the reformation of the parental defective molecules. Key:  $\equiv$ , deleted region;  $\blacksquare$ , genic region; djn, deletion-associated junction.

recreation of the wild-type genome. For example, the critical feature of the defective mtDNAs participating in the complementation event is that, in each case, one end of their deletions apparently overlaps, so that both molecules lack a common region. For ease of presentation, the case of overlapping deletion end-points is considered and the limiting case where deletion end-points coincide is discussed later. However, the importance of overlapping deletions to the direction of intramolecular recombination can be illustrated by first considering the example where there is no overlap or coincidence in deletion end-points. Recombination via homologous regions between two mtDNA molecules having nonoverlapping deletions leads to the formation of a molecule containing a duplicated region (Figure 11). Intramolecular homologous site recombination in part of this duplication (X) leads only to recreation of the defective mtDNAs; however, recombination across the other region leads to reformation of the wild-type molecule. Consequently, where this type of recombination is possible, the larger mitochondrial genome containing the du-

plication is not expected to persist over many generations. Indeed, we find that the major proportion of restored forms in complementation experiments do contain wild-type mtDNA (EVANS, OAKLEY and CLARK-WALKER 1985). Conversely, where deletion end-points overlap, one plane of homologous site recombination is lost and, as a consequence, it is impossible to form a molecule that in any way resembles the wild-type. Deletion end-point overlap is the probable basis for the persistence of the abnormal mtDNAs in hfp strains (see EVANS, OAKLEY and CLARK-WALKER 1985). Excision from such a molecule leads only to reformation of the original defective mtDNAs and this, we believe, is the basis for the high frequency of petite formation in these strains and for the nonoverlapping pattern of complementation when the resulting petites are crossed among themselves (CLARK-WALKER *et al.* 1976). This proposal is supported by data from an analysis of the mitochondrial genomes present in petites derived from hfp strains. The mtDNA in all such strains was found to be identical, by restriction endonuclease analysis, to either one or other of the hypothesized complementary defective genomes present in the hfp strains (R. J. EVANS and G. D. CLARK-WALKER, unpublished data).

Two observations from the results of studies on hfp strains need further comment. Although for ease of illustration and for the theoretical reasons outlined above we have described the pairs of defective but complementary mtDNA molecules in the hfp strains as containing overlapping deletions, our mapping studies are not precise enough to establish this point beyond doubt. Thus, for each hfp strain, both defective molecules have one of their deletion end-points in a common restriction fragment, and it is possible that such deletions could commence from a common site. The clarification of this point can be obtained by sequence determination across the novel junctions, and these studies have commenced. However, even if coincidence of deletion end-points is observed, such a result will not invalidate the idea that persistence of the hfp trait depends on the absence of a plane of recombination in the recombinant molecule. In terms of the model illustrated in Figure 11, deletion end-point coincidence can be viewed as a limiting case of deletion end-point overlap.

The second issue that carries a proviso concerns the postulated coexistence of the defective mtDNA molecules. In three of the four mapped hfp strains, one of the pair of defective mtDNA molecules is overrepresented. Although this result clearly indicates that one of the defective forms exists as a separate entity from the postulated recombinant molecule, we do not know the position of the equilibrium between the molecular species within the respiratory competent cell. Resolution of this question is complicated by the high proportion of petite mutants in hfp cultures. Aberrant ratios of defective mtDNAs within a culture could arise, therefore, from the separately located molecules from petite mutants and from coexisting defective molecules in respiratory competent cells. Irrespective of the true position of the equilibrium, it is possible to suggest a reason for aberrant ratios of mtDNA species by analogy with the explanation for suppressiveness of some petite mutants. For instance, the overrepresented species of defective mtDNA could have a faster replication

rate than the complementary molecule. These rates, may, in turn, be dictated by the presence or absence of particular sequences promoting replication. Candidates for such sequences could be the *ori/rep* regions known to be present in multiple copies in the *S. cerevisiae* mtDNA and to promote the replication of defective molecules in suppressive petite mutants (BLANC and DUJON 1980; DEZAMAROCZY *et al.* (1981).

The above interpretation of our results provides a viewpoint for considering the heterogeneous size distribution and nonstoichiometric levels of circular molecules found in plant mtDNAs (LEAVER and GRAY 1982; WALLACE 1982). For example, it has been suggested recently that a likely explanation for the tripartite arrangement of mtDNA in *Brassica campestris* is due to recombination via short, tandemly repeated sequences in a parental molecule to yield reciprocally deleted circular fragments (PALMER and SHIELDS 1984). If, in general, each of the deleted fragments, by analogy to the *hfp* mitochondrial genomes, has its own replication rate, then a complex pattern of nonstoichiometric fragments would be found in restriction endonuclease digests.

Mitochondrial genome organization in *mfp* strains differs fundamentally from that described for *hfp* strains. In the two mapped *mfp* strains, a pair of defective mtDNAs had undergone a site-specific recombination event to yield a recombinant molecule carrying a large inverted repeat. The elevated but not high frequency of petite formation in *mfp* strains cannot be ascribed to recombination via inverted duplicated regions, as this would merely lead to isomerization. Therefore, elevated levels of petite formation in *mfp* strains are perhaps a consequence of the particular sequences that are duplicated. As a result of the inversions, short repeated sequences of opposite orientation in the wild-type mtDNA would now be in the same orientation and, therefore, may offer additional opportunities for recombination leading to deletion. Such sequences may be the 300 base pairs (bp) *ori/rep* regions that confer replicative advantage on mtDNA in suppressive petite mutants (BLANC and DUJON 1980; DEZAMAROCZY *et al.* 1981) or the 50 or more G + C rich regions of 30–50 bp (PRUNELL and BERNARDI 1977). These two types of sequence element, together with short homologous sequences in A + T rich regions and oppositely orientated short repeated sequences have been implicated in the formation of petite mutants (MAROTTA *et al.* 1982; DEZAMAROCZY, FAUGERON-FONTY and BERNARDI 1983; SOR and FUKUHARA 1983).

The patterns produced on restriction endonuclease digestion of mtDNA from *hfp* strains [1]14.17s and [2]6.5s and *mfp* strains [1]16.6s and [1]16.17s proved too complex to interpret (see Figure 3 of the accompanying paper). In the case of the two *hfp* strains, each displayed more than two novel bands in digests, and frequently, several wild-type bands were absent. Relative stoichiometries of the bands present were hard to interpret. A possible explanation for these results comes from an extension of our model of *hfp* mitochondrial genome organization to one involving double deletions in one of the parental defective mtDNAs entering the cross. Consider, for example, the likely events upon recombination of a molecule having a single deletion with one containing two deletions, as depicted in Figure 12. The homologous recombination of

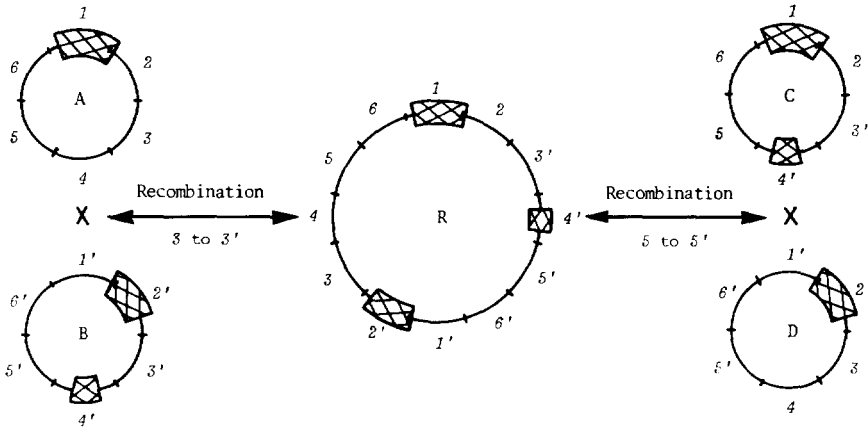
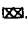


FIGURE 12.—The effect of a double deletion on the products of homologous recombination between defective mtDNA molecules. A recombinant heterodimer (R) formed by recombination between molecules A and B may, depending on the plane of intramolecular recombination, either regenerate the original molecules or produce two new forms, C and D. In the diagram a deletion is indicated by .

two defective molecules A and B through a co-retained region "3" leads to the formation of a recombinant heterodimer "R." Because of the presence of two regions of homology in R, alternative planes of recombination are available. Intramolecular recombination, therefore, may either reform the parental defective molecules A and B or create two new defective molecules C and D. In general, the number of possible rearrangements will depend on the number of secondary deletions sustained by either parental molecule. Although the presence of numerous forms would not in itself alter the restriction analysis, two complications may arise. One such complication is that each newly created defective molecule may have its own replication rate. Differential replication of numerous molecular species would cause major difficulties to mapping. The second complication concerns the position of restriction sites relative to a pair of novel junctions. Consider the example illustrated in Figure 13 that shows a section of a DNA molecule that has sustained two deletions. Depending on whether or not an enzymic cleavage site lies between the two deletions, one or two junctions will be detected in digests. Homologous recombination occurring in the region separating the deletions will not affect the size of junctions detected by enzyme y. This enzyme cleaves between the two excised sequences and although, as a result of the recombination, the deletions now lie on different molecules, the junction fragments are independent of each other and are unchanged. The effect of recombination on the junction detected by enzyme x, however, is the formation of two hybrid junctions by separating the deletions onto different molecules. This "hybridization" effect on junction fragments, especially when coupled with differential replication rates, is expected to complicate the interpretation of mtDNA restriction fragment data in strains containing multiple deletions. Although double deletions and their consequences may be sufficient to account for the complicated mi-

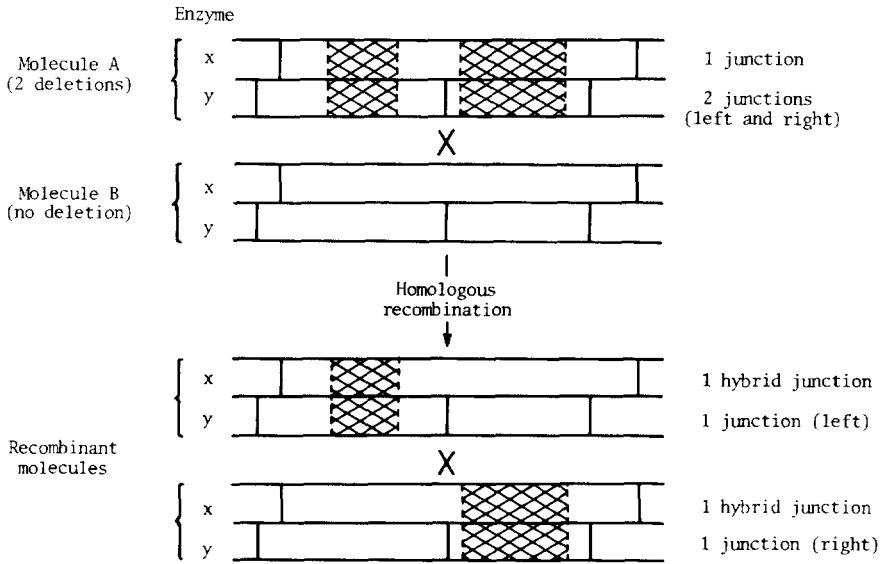


FIGURE 13.—Influence of the position of restriction sites (relative to a pair of junctions in a doubly deleted molecule) on the detection of “hybrid” junction fragments. The diagram is discussed in detail in the text. Deletions are indicated here by .

tochondrial genomes in strains [1]14.17s and [2]6.5s, we do not exclude the possibility of other explanations.

We could not establish the structure of the mitochondrial genomes in mfp strains [1]16.6s and [1]16.17s, as both mtDNAs appear to have duplicated junction fragments and substoichiometric bands. It is possible that there is a mixture of restored molecules in these strains that may have arisen from mixtures of defective mtDNAs in the original parental petites.

Consideration of the mapped genomes in hfp and mfp strains has led us to the view that the observed molecules could reflect the deleted mtDNAs in the petite mutants before complementation. This view is supported by the observation that the mitochondrial genome of hfp strains remains unchanged through successive subculture (EVANS, OAKLEY and CLARK-WALKER 1985) and suggests to us that an analysis of the mtDNA in strains restored to respiratory competence might provide a method of investigating the initial events in petite formation. This would provide a window on mtDNA organization in respiratory deficient mutants at a stage significantly earlier than has previously been possible, as such a study would not be dependent on the use of established petite strains that may have sustained secondary deletions.

Circumstantial support for the involvement of some form of *preferred* recombination sites in the *initial* deletion events in spontaneous petite formation comes from our mapping data from both hfp and mfp mtDNAs (Table 4, Figure 14a). Two regions that appear to be commonly involved in deletion end-points have been identified. One lies in the vicinity of the 5.5-kbp *HhaI* and 6.9-kbp *ClaI-HhaI* fragments that occur between the SrRNA gene and the

TABLE 4

Mitochondrial DNA fragments (kbp) containing deletion end-points

Strain	A. Site of deletion end-point				B. Site of overlap
	Molecule $\alpha$		Molecule $\beta$		
[1]9.6s3 } [1]9.25s }	2.35 (H)	4.80 (HP)	3.80 (HP)	4.80 (HP)	4.80 (HP)
[1]9.6s4	5.50 (H)	0.90 (BSp)	5.50 (H)	6.90 (CH)	5.50 (H)
[1]9.6s5	6.90 (CH)	4.35 (H)	4.80 (HP)	1.60 (CSp)	4.35 (H)/4.8 (HP)
[1]15.19S	4.35 (H)	3.50 (HHp)	6.90 (CH)	4.35 (H)	4.35 (H)
[2]13.10s	5.50 (H)	4.80 (HP)	5.50 (H)	4.10 (CH)	5.50 (H)
[2]17.5S	4.35 (H)	3.80 (PSP)	6.90 (CH)	4.35 (H)	4.35 (H)

D13.1A restriction fragments that are the site of deletion end-points in the defective mtDNAs of sectored strains (A) and deletion end-point overlaps between pairs of defective mtDNA molecules in sectored strains (B). The restriction fragments quoted are the smallest to which the deletion end-points or overlaps have been mapped, and the digests that yielded them are identified in parentheses. See legend to Figure 14 for restriction endonuclease name abbreviations. In the case of deletion end-point site, the left end-point is the first given.

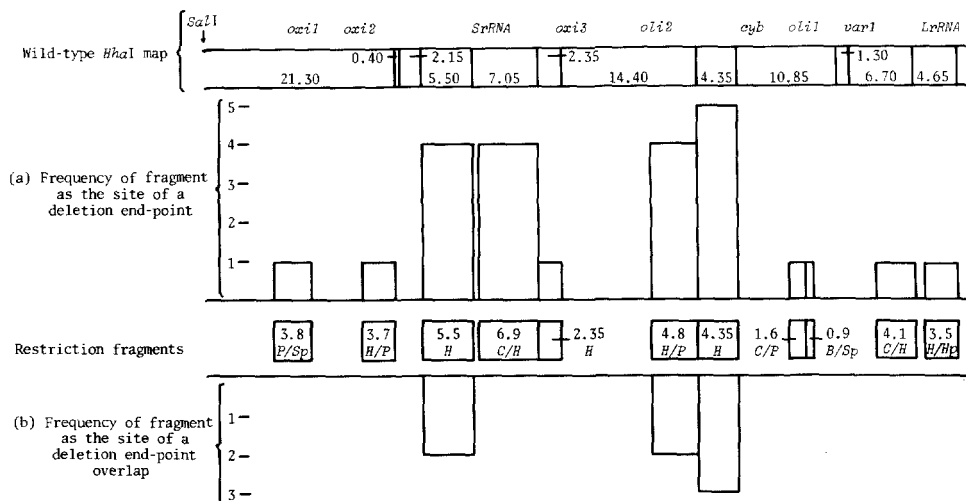


FIGURE 14.—Wild-type map position of deletion end-points (a) and deletion end-point overlaps (b) of the defective mtDNA molecules found in six sectored strains. Data have been taken from Table 4. In the case of strain [1]9.6s5, where the deletion end-point overlap could extend to two fragments, both are scored as being the site of an overlap. Fragment sizes are given in kilobase pairs. Restriction endonuclease names are abbreviated in the diagram: B = *Bam*HI, C = *Cla*I, H = *Hha*I, Hp = *Hpa*I, P = *Pvu*II, Sp = *Sph*I.

*oxi2* locus, while the other lies in the region of the 4.8-kbp *Hha*I-*Pvu*II fragment and the 4.35-kbp *Hha*I fragment between the *oli2* locus and the apocytochrome b gene. These two locations have also been identified by marker retention studies in petite mutants as bounding an area of the mitochondrial genome (encoding the *oxi3* and *oli2* loci) that is preferentially lost (FUKUHARA, MOUSTACCHI and WESOLOWSKI 1978; HEUDE, FUKUHARA and MOUSTACCHI 1979). However, our results carry the qualification that they are obtained from



hfp and mfp strains that are required to contain a full complement of genes, as well as some form of overlapping deletion.

The mapping studies have also revealed two areas of the mtDNA (Figure 14b) that may be eliminated from the mitochondrial genome without affecting respiratory activity. These correspond to regions of deletion end-point overlap and suggest that analysis of restored strains may have general application in identifying dispensible regions of mtDNA in *S. cerevisiae*. One lies in the segment between the *oli2* and *cyb* genes, and it must be concluded that this sequence is not needed for respiratory competence under the conditions in which the strains were grown. It may be significant that a 1.8-kbp optional sequence has been reported in this region of a wild-type mitochondrial genome (COBON *et al.* 1982). This variation has no apparent effect on respiratory function and establishes that deletions can be tolerated in this part of the mtDNA molecule. The other, apparently dispensable, region lies upstream from the gene encoding the small ribosomal RNA.

We thank R. A. BUTOW for the plasmid pBRvar1, P. NAGLEY for petite 68-4-2, H. FUKUHARA for petite strain P2 and A. TZAGOLOFF for the remaining petites used in the hybridization studies. R. J. EVANS acknowledges the receipt of a Ph.D. scholarship from the Australian National University, Canberra.

#### LITERATURE CITED

- ATCHISON, B. A., K-B. CHOO, R. J. DEVENISH, A. W. LINNANE and P. NAGLEY, 1979 Biogenesis of mitochondria. 53. Physical map of genetic loci in the 21s ribosomal RNA region of mitochondrial DNA in *Saccharomyces cerevisiae*. *Mol. Gen. Genet.* **174**: 307-316.
- BLANC, H. and B. DUJON, 1980 Replicator regions of the yeast mitochondrial DNA responsible for suppressiveness. *Proc. Natl. Acad. Sci. USA* **77**: 3942-3946.
- BONITZ, S., G. CORUZZI, B. THALENFELD and A. TZAGOLOFF, 1980 Assembly of the mitochondrial membrane system: structure and nucleotide sequence of the gene coding for subunit 1 of yeast cytochrome oxidase. *J. Biol. Chem.* **255**: 11927-11941.
- CLARK-WALKER, G. D., C. R. MCARTHUR and K. S. SRIPRAKASH, 1983 Order and orientation of genic sequences in circular mitochondrial DNA from *Saccharomyces exiguus*: implications for evolution of yeast mtDNAs. *J. Mol. Evol.* **19**: 333-341.
- CLARK-WALKER, G. D. and G. L. MIKLOS, 1975 Complementation in cytoplasmic petite mutants of yeast to form respiratory competent cells. *Proc. Natl. Acad. Sci. USA* **72**: 372-375.
- CLARK-WALKER, G. D., K. M. OAKLEY, C. R. MCARTHUR and G. L. MIKLOS, 1976 High spontaneous petite frequency strains of *Saccharomyces cerevisiae* generated in complementation tests. pp. 491-495. In: *Genetics and Biogenesis of Chloroplasts and Mitochondria*, Edited by T. BUCHER, W. NEUPERT, W. SEBALD and S. WERNER. North-Holland Biomedical Press, Amsterdam.
- CLARK-WALKER, G. D. and K. S. SRIPRAKASH, 1981 Sequence rearrangements between mitochondrial DNAs of *Torulopsis glabrata* and *Kloeckera africana* identified by hybridization with six polypeptide encoding regions from *Saccharomyces cerevisiae* mitochondrial DNA. *J. Mol. Biol.* **151**: 367-387.
- CLARK-WALKER, G. D., K. S. SRIPRAKASH, C. R. MCARTHUR and A. A. AZAD, 1980 Mapping of mitochondrial DNA from *Torulopsis glabrata*. Location of ribosomal and transfer RNA genes. *Curr. Genet.* **1**: 209-217.
- COBON, G. S., M. W. BEILHARZ, A. W. LINNANE and P. NAGLEY, 1982 Biogenesis of mitochondria: mapping of transcripts from the *oli2* region of mitochondrial DNA in two grande strains of *Saccharomyces cerevisiae*. *Curr. Genet.* **5**: 97-107.

- DANIELS, D. L., J. L. SCHROEDER, F. R. BLATTNER, W. SZYBALSKI and F. SANGER, 1983 Appendix. In: *Lambda II*, Edited by R. W. HENDRIX, J. W. ROBERTS, F. W. STAHL AND R. A. WEISBERG. Cold Spring Harbor Laboratory, Cold Spring Harbor, New York.
- DEZAMAROCZY, M., R. MAROTTA, G. FAUGERON-FONTY, R. GOURSOT, M. MANGIN, G. BALDACCI and G. BERNARDI, 1981 The origins of replication in the yeast mitochondrial genome and the phenomenon of suppressivity. *Nature* **292**: 75-78.
- DEZAMAROCZY, M., G. FAUGERON-FONTY and G. BERNARDI, 1983 Excision sequences in the mitochondrial genome of yeast. *Gene* **21**: 193-202.
- EVANS, R. J., 1983 Investigation of high frequency petite-forming strains of *Saccharomyces cerevisiae*. Ph.D. Thesis, Australian National University, Canberra.
- EVANS, R. J., K. M. OAKLEY and G. D. CLARK-WALKER, 1985 Elevated levels of petite formation in strains of *Saccharomyces cerevisiae* restored to respiratory competence. I. Association of both high and moderate frequencies of petite mutant formation with the presence of aberrant mitochondrial DNA. *Genetics* **111**: 389-402.
- FUKUHARA, H., E. MOUSTACCHI and M. WESOLOWSKI, 1978 Preferential deletion of a specific region of mitochondrial DNA in *Saccharomyces cerevisiae* by ethidium bromide and 3-carbethoxy-psoralen. *Mol. Gen. Genet.* **162**: 191-201.
- GREENE, P. J., H. L. HEYNEKAR, F. BOLIVAR, R. L. RODRIGUEZ, M. C. BETLACH, A. A. COVARUBIAS, K. BACKMAN, D. J. RUSSELL, R. TAIT and W. BOYER, 1978 A general method for the purification of restriction enzymes. *Nucleic Acids Res.* **5**: 2373-2380.
- HEUDE, M., H. FUKUHARA and E. MOUSTACCHI, 1979 Spontaneous and induced *rho* mutants of *Saccharomyces cerevisiae*: patterns of loss of mitochondrial genetic markers. *J. Bacteriol.* **139**: 460-467.
- HUDSPETH, E. S., W. M. AINLEY, D. S. SHUMARD, R. A. BUTOW and L. I. GROSSMAN, 1982 Location and structure of the *var1* gene on yeast mitochondrial DNA: nucleotide sequence of the 40.0 allele. *Cell* **30**: 617-626.
- LEAVER, C. J. and M. W. GRAY, 1982 Mitochondrial genome organisation and expression in higher plants. *Annu. Rev. Plant Physiol.* **33**: 373-402.
- MACINO, G. and A. TZAGOLOFF, 1979 Assembly of the mitochondrial membrane system: the DNA sequence of a mitochondrial ATPase gene in *Saccharomyces cerevisiae*. *J. Biol. Chem.* **254**: 4617-4623.
- MACINO, G. and A. TZAGOLOFF, 1980 Assembly of the mitochondrial membrane system: sequence analysis of a yeast mitochondrial ATPase gene containing the *oli-2* and *oli-4* loci. *Cell* **20**: 507-517.
- MAROTTA, R., Y. COLIN, R. GOURSOT and G. BERNARDI, 1982 A region of extreme instability in the mitochondrial genome of yeast. *EMBO J.* **1**: 529-534.
- NOBREGA, F. and A. TZAGOLOFF, 1980 Assembly of the mitochondrial membrane system: DNA sequence and organisation of the cytochrome b gene in *Saccharomyces cerevisiae* D273-10B. *J. Biol. Chem.* **255**: 9828-9837.
- OAKLEY, K. M. and G. D. CLARK-WALKER, 1978 Abnormal mitochondrial genomes in yeast restored to respiratory competence. *Genetics* **90**, 517-530.
- O'FARRELL, P. H., E. KUTTER and M. NAKANISHI, 1980 A restriction map of the bacteriophage T4 genome. *Mol. Gen. Genet.* **179**: 421-435.
- PALMER, J. D. and C. R. SHIELDS, 1984 Tripartite structure of the *Brassica campestris* mitochondrial genome. *Nature* **307**: 437-440.
- PRUNELL, A. and G. BERNARDI, 1977 The mitochondrial genome of wild-type yeast cells. VI. Genome organisation. *J. Mol. Biol.* **110**: 53-74.
- SOR, F. and H. FUKUHARA, 1980 Séquence nucléotidique du gène de l'ARN ribosomique 15s mitochondrial de la levure. *C. R. Acad. Sc. Paris. Ser. D.* **291**: 933-936.

- SOR, F. and H. FUKUHARA, 1983 Unequal excision of complementary strands is involved in the generation of palindromic repetitions of rho- mitochondrial DNA in yeast. *Cell* **32**: 391-396.
- SUTCLIFFE, J. G., 1978 pBR322 restriction map derived from the DNA sequence: accurate DNA size markers up to 4361 nucleotide pairs long. *Nucleic Acids Res.* **5**: 2721-2728.
- THALENFELD, B. and A. TZAGOLOFF, 1980 Assembly of the mitochondrial membrane system: sequence of the *oxi2* gene of yeast mitochondrial DNA. *J. Biol. Chem.* **255**: 6173-6180.
- WALLACE, D. C., 1982 Structure and evolution of organelle genomes. *Microbiol. Rev.* **46**: 208-240.

Communicating editor: I. HERSKOWITZ

APPENDIX 1

*Sizes of restriction endonuclease fragments from mtDNA of [1]15.19s*

Band	<i>HhaI</i>		<i>BamHI/HhaI</i>		<i>Clal/HhaI</i>		<i>Clal/PvuII</i>		<i>HhaI/HpaI</i>	
	A	B	A	B	A	B	A	B	A	B
1	21.30	3	21.30	3	21.30	3	21.05	2	21.30	3
2	14.40	1	10.75	1	14.40	1	~19*	1	14.20	1
3	10.85	2	6.60	1	6.90	1	11.90	3	7.05	1
4	7.05	1	5.50	3	5.60	2	10.60*	2	6.60	2
5	6.70	2	5.45	2	5.50	3	9.50	2	5.50	3
6	5.50	3	5.00	2	5.35*	2	8.90	1	5.50*	2
7	5.50*	2	4.95*	2	5.25	2	7.95	1	4.85	2
8	4.65	2	4.65	2	4.65	2	5.30	3	4.25	2
9	2.35	1	3.65	1	4.10	2	2.00	1	3.50	2
10	2.15	3	3.10	2	2.60	2	~171.75		2.20	1
11	2.15*	1	2.75	2	2.15	3			2.15*	1
12	1.30	2	2.35	1	2.15*	1			1.85	2
	0.40	(3)	2.15	3	2.00	1			1.35	3
	172.00		2.15*	1	1.30	2			1.30	2
			1.30	2	0.40	(3)			1.15	2
			1.25	2	0.35	(1)			0.80	(3)
			0.55	(3)	0.15	(3)			0.40	(3)
			0.40	(3)	172.00				0.20	(1)
			172.00						0.15	(1)
									172.00	

Fragment sizes, in kbp, are shown in column A, and relative band stoichiometries determined by densitometry are given in column B. The total given below each column A takes into account both size and observed stoichiometry of the individual fragments. As a consequence, this total does not represent the mitochondrial genome size for the strain; see main text. In Appendixes 1-3, the band numbers given for *HhaI* fragments refer to the peaks shown in Figure 3c, d and e of the main text. Novel fragments are marked as \*, and parentheses indicate that the stoichiometries have been estimated from the known map positions of these fragments (relative to regions of established stoichiometry).

## APPENDIX 2

*Sizes of restriction endonuclease fragments from mtDNA of [2]13.10s*

Band	<i>HhaI</i>		<i>ClaI</i>		<i>ClaI/HhaI</i>		<i>ClaI/PvuII</i>		<i>HhaI/PvuII</i>	
	A	B	A	B	A	B	A	B	A	B
1	21.30	2	large*	—	21.30	2	21.05	2	12.30	2
2	14.40	1	24.35	1	14.40	1	~18.50*	2	10.85	3
3	10.85	3	9.50	3	6.90	1	14.40	1	7.70*	1
4	7.70*	1	8.90	1	5.60	3	9.50	3	7.60	1
5	7.05	1	5.30	2	5.25	3	8.90	1	7.05	1
6	6.70	2	5.25*	1	5.10*	1	7.95	1	6.70	2
7	4.65	2	—		4.65	2	5.30	2	5.30	2
8	4.35*	3			4.35	3	5.25*	1	4.80	1
9	2.60	2			4.10	2	2.00	1	4.65	2
10	2.35	1			2.60	3	~156.70		4.35	3
11	2.15	2			2.60*	2			3.70	2
12	1.30	3			2.15	2			2.60*	2
	0.40	(2)			2.00	1			2.35	1
	156.60				1.30	3			2.15	2
					0.40	(2)			2.00	1
					0.35	(1)			1.30	3
					0.15	(1)			0.40	(2)
					156.60				156.60	

Fragment sizes, in kbp, are shown in column A, and relative band stoichiometries determined by densitometry are given in column B. In Appendixes 1–3, the band numbers given for *HhaI* fragments refer to the peaks shown in Figure 3c, d and e of the main text. Novel fragments are marked as \*, and parentheses indicate that the stoichiometries have been estimated from the known map positions of these fragments (relative to regions of established stoichiometry).

APPENDIX 3

Sizes of restriction endonuclease fragments from mtDNA of [2]17.5s

Band	<i>HhaI</i>		<i>BamHI/PvuII</i>		<i>Clal/HhaI</i>		<i>Clal/PvuII</i>		<i>HhaI/PvuII</i>	
	A	B	A	B	A	B	A	B	A	B
1	21.30	2	22.40	2	21.30	2	21.05	2	12.30	2
2	14.40	1	12.50	1	14.40	1	11.90	3	10.85	2
3	12.20*	1	12.30	3	12.20*	1	11.60*	2	7.60	1
4	10.85	2	8.70*	2	6.90	1	9.50	2	7.05	1
5	7.05	1	8.00*	1	6.35*	2	8.90	1	6.70	2
6	6.70	2	5.65	2	5.60	2	8.00*	1	6.50*	2
7	6.50*	2	5.30	3	5.50	3	7.95	1	5.50	3
8	5.50	3	5.00	2	5.25	2	5.30	3	5.30	3
9	4.65	2	3.95	1	4.65	2	2.00	1	4.80	1
10	2.35	1	2.00	1	4.10	2	162.75		4.65	2
11	2.15	3	162.75		2.60	2			3.70	3
12	1.30	2			2.15	3			3.20*	1
	0.40	(3)			2.00	1			2.35	1
	162.75				1.30	2			2.15	3
					0.40	(3)			2.00	1
					0.35	(1)			1.30	2
					0.15	(3)			0.40	(3)
					162.75				162.75	

Fragment sizes, in kbp, are shown in column A, and relative band stoichiometries determined by densitometry are given in column B. In Appendixes 1-3, the band numbers given for *HhaI* fragments refer to the peaks shown in Figure 3c, d and e of the main text. Novel fragments are marked as \*, and parentheses indicate that the stoichiometries have been estimated from the known map positions of these fragments (relative to regions of established stoichiometry).

## APPENDIX 4

*Sizes of restriction endonuclease fragments from mtDNA of [1]9.6s4*

<i>Bam</i> HI/ <i>Cla</i> I		<i>Bam</i> HI/ <i>Hha</i> I		<i>Bam</i> HI/ <i>Sph</i> I		<i>Cla</i> I/ <i>Pvu</i> II		<i>Cla</i> I/ <i>Sph</i> I		<i>Hha</i> I/ <i>Sph</i> I	
A	B	A	B	A	B	A	B	A	B	A	B
large*	1	21.30	1	18.60	1	21.05	1	20.00	2	14.40	2
17.85	2	10.75	2	~18.0*	1	14.40	2	~18.0*	1	12.80	1
8.65*	1	6.50	1	16.35	2	10.25*	1	17.25	1	8.50	1
8.50	1	6.50*	1	9.40*	1	9.50	1	8.90	1	7.05	1
5.65	1	6.50*	1	8.85	1	8.90	1	8.65*	1	6.70	1
4.00	2	5.45	1	5.65	1	8.65*	1	7.90	1	6.50*	1
2.50	2	5.00	1	4.10	2	7.95	2	4.00	2	5.60	2
2.50	1	4.65	1	3.65	2	5.30	1	1.60	2	4.65	1
1.35	1	4.35	2	1.50	2	2.00	2	0.35	(2)	4.35	2
0.40	1	3.65	2	0.90	(1)	112.35		~112.65		4.00	1
—		3.10	1	~112.60						2.40*	1
		2.75	2							2.35	2
		2.35	2							2.15	1
		2.15	1							1.30	1
		1.30	1							1.25	2
		1.25	1							0.40	(1)
		0.55	(1)							112.65	
		0.40	(1)								
		112.35									

Fragment sizes, in kbp, are shown in column A, and relative band stoichiometries determined by densitometry are given in column B. Novel fragments are marked as \*, and parentheses indicate that the stoichiometries have been estimated from the known map positions of these fragments (relative to regions of established stoichiometry).